Enzymatic and Physical Characterization of Diacylglycerol–Phosphatidylcholine Interactions in Bilayers and Monolayers†

Beth A. Cunningham, Takahiro Tsujita,‡ and Howard L. Brockman*
The Hormel Institute, The University of Minnesota, Austin, Minnesota 55912
Received June 23, 1988; Revised Manuscript Received August 19, 1988

ABSTRACT: The miscibility of 1,3-dioleoylglycerol (DOG) with 1-stearoyl-2-oleoylphosphatidylcholine (SOPC) and 1-palmitoyl-2-oleoylphosphatidylcholine (POPC) dispersed in excess buffer was characterized by physical and enzymatic methods. Thermograms for all SOPC–DOG mixtures exhibit a transition at 5.3 °C. Above 0.25 mole fraction of DOG, metastability is observed; after the first scan, a second peak appears at 23.4 °C which corresponds to the chain melting of pure DOG. This suggests that a complex or preferred packing array is formed which has a DOG mole fraction of 0.25 (X_c). Bilayer morphology is maintained in the metastable state up to 0.8 mole fraction of DOG. Above 0.8, a novel, nonlamellar phase is formed. Fluorescence polarization of 1,6-diphenylhexatriene shows that, relative to SOPC alone, there is little change in the order of the acyl chains up to X_c followed by a large decrease above X_c. Similar results were obtained using POPC. Miscibility was also studied in lipid films at the argon–buffer interface. Isothermal phase diagrams for the mixtures at 15 and 24 °C exhibited phosphatidylcholine–DOG complex formation, a region of phosphatidylcholine and complex coexistence, and a region of complex and DOG miscibility. The mole fractions of DOG in the complex (X_c) range from 0.24 to 0.27. Porcine pancreatic phospholipase A_2 and pancreatic lipase plus colipase were used as probes of the surface in both the monolayer and bilayer systems. In both systems and with both enzymes, substrate hydrolysis increased abruptly with increasing DOG. Overall, the formation of a complex at the same mole fraction of DOG in bilayers as in monolayers and the similar regulation of lipolytic enzyme activity in both systems suggest that the structures of DOG–phosphatidylcholine monolayers and bilayers are governed by a similar lipid–lipid interaction.

Diacylglycerols have several major roles in cellular processes. Of particular interest is the generation of diacylglycerol in response to extracellular signals. Although not normally present in large quantities in membranes, they are the product of the hydrolysis of inositol phospholipids (Berridge & Irvine, 1984; Majerus et al., 1984; Nishizuka, 1986), and possibly phosphatidylcholine (PC)[1] (Cabot et al., 1988), by phospholipase C. These diacylglycerols, in turn, activate protein kinase C, a calcium- and phospholipid-dependent enzyme, during cell surface signal transduction (Nishizuka, 1986). Kolesnick and colleagues have shown that 1,2-diacylglycerols stimulate the degradation of PC by phospholipase A_2 (Kolesnick & Paley, 1987) and sphingomyelin by sphingomyelinase (Kolesnick, 1987) in rat pituitary cells and that these events occur independently of protein kinase C. In a similar study, diacylglycerol stimulation of phospholipase A_2 from Swiss 3T3 fibroblasts was not affected by inhibition of protein kinase C (Burch, 1988). It has also been recently reported that 1,2-diacylglycerols, but not phorbol esters, activate a potential inhibitory pathway for protein kinase C in pituitary cells (Kolesnick & Clegg, 1988). These observations show that not all regulatory effects of diacylglycerols are mediated through protein kinase C, i.e., that other mechanisms must be operative.

One possible consequence of localized or global diacylglycerol production in cells is to alter the structure and packing of membrane phospholipids, such as PC. Several studies have indicated that diacylglycerols incorporated into phosphatidylcholine bilayers cause major structural and stability changes (Das & Rand, 1984, 1986; Dawson et al., 1984); at low concentrations, they spread apart the polar headgroups, whereas at high concentrations they induce hexagonal and cubic phases. The miscibility behavior of DOG with POPC has been studied in films at the argon/buffer interface (Smaby & Brockman, 1985). It formed a complex with POPC at a mole fraction of DOG of 0.25. Recent findings from this laboratory (Wolfe & Brockman, 1988) have strengthened the idea that monolayers and bilayers share some physical properties and that information about one state can be translated to the other. This prompted us to compare physically the miscibility characteristics of DOG and PC in aqueous dispersion and in lipid films. The 1,3-isomer was used because of its stability and because earlier data (Smaby & Brockman, 1985) show that in monolayers the 1,2- and 1,3-isomers behaved similarly. To further investigate the structural relationship between lipids in these two states, we used lipolytic enzymes as probes of surface organization. The results indicate that a complex, i.e., a preferred packing array, is formed at the same mole fraction of DOG in bilayers as in monolayers and that lipolytic enzyme activity is regulated in a similar manner in both states.

Materials and Methods

Lipids. POPC and SOPC were purchased from Avanti Biochemicals (Birmingham, AL), and DOG was purchased from NuChek Prep, Inc. (Elysian, MN). [*Oleoyl*-1-^{14}C]-1-palmitoyl-2-oleoylphosphatidylcholine and [*dioleoyl*-1-^{14}C]-dioleoylphosphatidylcholine were obtained from New England Nuclear (Boston, MA). 1,3-[1-^{14}C]Dioleoylglycerol was prepared by isomerization of 1,2-[1-^{14}C]-dioleoylglycerol

†This research was supported by USPHS–NIH Grants HL08214 and HL07311 (B.A.C.) and by the Hormel Foundation.
‡Present address: Ehime University School of Medicine, Department of Medical Biochemistry, Shigenobu, Ehime 791-02, Japan.

[1] Abbreviations: PC, phosphatidylcholine; POPC, 1-palmitoyl-2-oleoyl-*sn*-glycero-3-phosphocholine; SOPC, 1-stearoyl-2-oleoyl-*sn*-glycero-3-phosphocholine; DPH, 1,6-diphenyl-1,3,5-hexatriene; DOG, 1,3-dioleoylglycerol; PLA_2, porcine pancreas phospholipase A_2.

0006-2960/89/0428-0032$01.50/0 © 1989 American Chemical Society

prepared from 50 μCi of [1-^{14}C]dioleoyl-*sn*-glycero-3-phosphocholine (specific activity 114 μCi/mol). [1-^{14}C]-Dioleoyl-*sn*-glycero-3-phosphocholine was dissolved in 1.0 mL of diethyl ether, and to this solution was added 1.0 mL of Tris-HCl (0.2 M, pH 7.3) containing 12 mM $CaCl_2$ and 0.15 mL of phospholipase C (250 units). After the solution was stirred for 2 h at room temperature, [1-^{14}C]dioleoylglycerol was extracted 3 times with 3 mL of hexane. The solvent was evaporated with N_2, and the lipid was dissolved in 2 mL of hexane to which 50 μL of 6 N HCl and 250 mg of silica gel 60 (E. Merck, Darmstadt, Germany) were added. After the mixture was stirred for 2 h at room temperature, lipids were extracted 3 times with 3 mL of chloroform/methanol (2:1). Following analytical thin-layer chromatography, 70% of the radioactivity migrated with authentic 1,3-DOG with the remainder as 1,2-DOG (26%) and oleic acid (3%). The 1,3-[1-^{14}C]dioleoylglycerol was purified by isocratic, high-performance liquid chromatography using a silica gel column (SILICA, Spheri-5, 4.6 × 30 mm; Brownlee Labs, Inc., Santa Clara, CA) with 0.4% ethanol in hexane as the solvent. Isomeric purity of the product was ≥99% and did not change with storage at −20 °C during the course of this study. Chemical and radiolabel purity of each lipid was determined by thin-layer chromatography. For unlabeled lipids, plates were treated with sulfuric acid and charred. Chemical purity was assessed by visual comparison of impurity spots, if any, with standards of known mass. The extent of impurities in radiolabeled lipids was determined by using a Berthold LB 2842 thin-layer chromatography linear analyzer (Wildbad, West Germany) equipped with a standard LB 2821 detector. An IBM PC/AT was employed for data acquisition and analysis. From detection limits, all lipids were shown to be greater than 99% pure.

Reagents. Ethanol was distilled from KOH and zinc (Perrin et al., 1966), and hexane (non-spectrograde) was from Burdick and Jackson Laboratories, Inc. (Muskegon, MI). The absence of surface-active impurities in solvents was determined as described earlier (Smaby et al., 1983). Water was purified by reverse osmosis, mixed-bed deionization, adsorption on activated charcoal, and filtration through a 0.22-μm Durapore membrane (Millipore Corp., Bedford, MA). Before use, buffers were filtered through a Diaflo hollow fiber with a molecular weight cutoff of 10 000 (Amicon Corp., Danvers, MA), degassed, and stored under argon. DOG was dissolved in hexane, and phospholipids were dissolved in hexane containing 5% ethanol (v/v). Phospholipid concentration was determined by assaying aliquots for organic phosphorus (Bartlett, 1959). All other chemicals were of reagent grade and used without further purification.

Proteins. Phospholipase C, type V, from *Bacillus cereus* (EC 3.1.4.3) and PLA_2 (phosphatidylcholine 2-acylhydrolase, EC 3.1.1.4, M_r 14 000) were obtained from Sigma Chemical Co. (St. Louis, MO). PLA_2 was desalted on a 1.6 × 20.0 cm column packed with GH25 (Amicon Corp.). A sample of 3.5 μg of PLA_2 appeared as a single band when subjected to electrophoresis on a 10–20% acrylamide gradient minigel (Jule Inc., New Haven, CT) followed by silver staining using the procedure of Morrissey (1981). PLA_2 activity was measured by using a pH stat assay as described previously (de Haas et al., 1968). Protein concentration for PLA_2 was determined by using an $E^{1\%}$ of 13.0 at 280 nm (Nieuwenhuizen et al., 1974). By use of these assays for protein concentration and activity, the PLA_2 preparation was found to have a specific activity of 793 units/mg, where 1 unit of activity is 1 μmol of fatty acid released per minute at 40 °C.

Colipase was purified from porcine pancreas as described previously (Canioni et al., 1977) in the presence of 2 mM benzamidine hydrochloride, 2 mM hydrocinnamic acid, and 0.5 mM N^{α}-benzoyl-D,L-arginine to inhibit protease activities (Chapus et al., 1981). One-milliliter aliquots (2.5 mg) of this preparation were then chromatographed on a MONO-Q HR 5/5 column (Pharmacia; Piscataway, NJ) using a 15-mL gradient, 0–0.15 M sodium chloride in 20 mM Tris, pH 8.0. The colipase obtained had a specific activity of 34 000 units/mg.

Partially purified lipase (triacylglycerol acylhydrolase, EC 3.1.1.3, M_r 52 000) was obtained by gel filtration on Sephacryl S200 (Pharmacia) of an extract from porcine pancreas as previously described (Rudd et al., 1987). All steps except those specified were performed at 4 °C. The fractions containing pancreatic lipase activity were combined, adjusted to pH 6.8, and made 1 mM in diisopropyl fluorophosphate. The enzyme was concentrated by precipitation with *tert*-butyl alcohol (1.4 volume of *tert*-butyl alcohol/H_2O, 95:5 v/v), and the resulting pellet was resuspended in 35 mL of 25 mM Bis-Tris, pH 6.0, containing protein inhibitors (Chapus et al., 1981) as described above. After centrifugation to remove insoluble material, the sample was applied to a 2.5 × 12.5 cm column of Fast Flow Q Sepharose (Pharmacia) equilibrated in the above buffer. The column was washed with 300 mL of buffer and the lipase eluted with a 1.3-L gradient, 0–0.25 M in sodium chloride. The fractions containing lipase activity were combined, adjusted to pH 6.5, and loaded on a 2.5 × 13 cm column of HA Ultragel–hydroxylapatite (LKB Instruments, Piscataway, NJ) equilibrated with 10 mM potassium phosphate, pH 6.5, containing 1 mM β-mercaptoethanol and 0.04% sodium azide and saturated with calcium chloride. After the column was washed with 1.5 L of equilibration buffer, lipase was eluted by stepping the buffer concentration up to 250 mM. Finally, residual colipase activity (~5%) was removed by gel filtration at 24 °C on a 21.5 × 37.5 cm TSK 3000 SW column (Toyosoda), flow rate 0.5 mL/min, equilibrated with 10 mM potassium phosphate, pH 6.8, containing 100 mM sodium chloride. The lipase obtained had a specific activity of 10 000 units/mg, and the ratio of colipase activity to lipase activity in the preparation was <0.01.

During purification, lipase and colipase activities were measured by using a modification of a pH stat assay described previously (Momsen & Brockman, 1978). Substrate was made by sonication for 5–10 min of 1 mL of tributyrin with 30 mL of 1 mM Tris buffer, pH 7, containing 0.15 M sodium chloride, 1 mM calcium chloride, 6 mM sodium taurodeoxycholate, 0.5% Brij 35 (w/v), and 0.02% sodium azide. The titrant was 50 mM sodium hydroxide. One unit of activity is 1 μmol of fatty acid released per minute at 25 °C. Lipase was assayed in the presence of 15 units of purified colipase, and colipase was assayed in the presence of 12 units of essentially colipase-free lipase. Protein concentration was determined by the absorbance at 280 nm using an $E^{1\%}$ of 13.3 for lipase (Verger et al., 1971) and 4.0 for colipase (Erlanson & Borgström, 1972).

Surface Pressure–Area Measurements. For physical characterization of lipid films, surface pressure–area isotherms were measured by using a fully automated Langmuir film balance system (Brockman et al., 1980, 1984). All films were spread from 51.67 μL of solvent onto a subphase of 0.01 M potassium phosphate/0.1 M sodium chloride, pH 6.6, at 15 and 24 °C. After standing at a large molecular area for 4 min, the films were compressed at ≤4 Å^2 min^{-1} molecule^{-1}. Phase transitions were identified by using second and third deriva-

tives, as previously described (Brockman et al., 1980).

Preparation of Lipid Dispersions. SOPC or POPC and DOG stock solutions were mixed together in the desired molar ratios, and the solvents were evaporated under a stream of nitrogen. Trace amounts of [^{14}C]POPC or [^{14}C]DOG were included in samples to be subjected to enzymatic hydrolysis. For fluorescence polarization measurements, DPH (Molecular Probes, Inc., Eugene, OR) was added at a lipid to DPH mole ratio of 500:1. After being subjected to high vacuum overnight, the lipid mixture was suspended in buffer, vortexed for 2 min at approximately 50 °C, incubated at 50 °C for 3 min, and sonicated at 50 °C in a bath sonicator (Branson 2200R-4) for 2 min. This vortex/sonicate cycle was then repeated twice. Phospholipid concentration in the lipid dispersions ranged from 2.0 to 26.4 mM depending on the type of experiment. Lipid composition was established by checking samples which had trace amounts of radiolabeled POPC and DOG. The mole fraction was determined from thin-layer chromatography as described previously and agreed to within 4% (relative). Experiments involving these dispersions were initiated within 5 min after their preparation unless specified otherwise.

Calorimetry. Thermotropic phase behavior of the DOG–SOPC and DOG–POPC lipid dispersions was studied by using a high-resolution MC-2 scanning microcalorimeter (MicroCal Co., Amherst, MA). Sample and buffer solution reference were delivered to the respective cells by syringe, and the cells were tightly sealed. The calorimeter cells were then equilibrated near 0 °C before measurements were taken. DSC thermograms were recorded during heating of the samples with a scan rate of 10 °C/h. After the first scan, the sample and reference were reequilibrated near 0 °C and rescanned. This process was repeated, usually 2 or 3 times, until consecutive scans were identical. Variations in buffer composition or the presence of $CaCl_2$ did not affect transition temperatures or enthalpies. Transition peak areas were obtained by cutting and weighing. The peak of the thermogram was used as the transition temperature.

Electron Microscopy. Lipid dispersions were characterized by transmission electron microscopy after freeze–fracture. Glycerol (25% v/v) was added after the dispersions were prepared in 50 mM PIPES, 100 mM NaCl, 2.5 mM $CaCl_2$, and 0.04% NaN_3 (pH 6.6) as described above. A drop of sample was placed on a 3-mm cup-type specimen holder and equilibrated at 15 °C. The sample was cryofixed by immersion in liquid nitrogen cooled freon and transferred to a Balzer BAF 300/301 apparatus. Immediately following the fracture, the sample was coated from a carbon/platinum electrode at a 45° angle, and a layer of carbon was deposited from a vertical electrode. Replicas were removed from the specimen holder by floating in distilled water, cleaned with chloroform/methanol, and placed on a 200-mesh copper grid (E. F. Fullam, Inc., New York, NY). The micrographs were taken with a JEOL 100S electron microscope at 60 kV at magnifications of up to 40000×.

Fluorescence Polarization. Steady-state fluorescence polarization of DPH was measured 90° relative to the exciting beam using an SLM-8000 spectrofluorometer. Polarizers supplied by SLM were used to polarize both the exciting and emitting beams. DPH was excited at 366 nm and fluorescence measured at 430 nm using a 399-nm Schott KV cutoff filter to reduce scattered light. The fluorescence polarization, P, was calculated according to (Shinitzky et al., 1971) $P = (I_{\parallel} - I_{\perp})/(I_{\parallel} + I_{\perp})$ where $I_{\parallel}$ and $I_{\perp}$ are observed intensities measured with polarizers parallel and perpendicular to the vertically polarized exciting beam, respectively. The SLM-8000 was interfaced to a microcomputer system to allow for manipulation and plotting of data. Measurements were made after equilibration of the sample in the cuvettes for 15 min at 15 ± 1.0 °C. No changes in polarization occurred after an additional 40 min.

Hydrolysis of Lipid Dispersions with Enzymes. Incubations were carried out with lipids dispersed as above in 50 mM PIPES buffer, pH 6.6, containing 100 mM NaCl and 0.04% NaN_3. The buffer also contained 2.5 mM $CaCl_2$ for dispersions incubated with PLA_2. After equilibration of the dispersions at 15 °C for 10–15 min, the reaction was initialized by the addition of enzyme. All reactions were carried out at 15 °C. For measurements of [^{14}C]DOG hydrolysis by lipase, aliquots of POPC–DOG dispersions were preincubated with 226 units of colipase for 2 min before the addition of 18.5 units of lipase. The final volume was 76 μL, and the final concentration of POPC was 3.7 mM. The reaction was terminated after 10 min by the addition of 300 μL of chloroform/methanol (1:2 v/v), thereby forming a one-phase system (Bligh & Dyer, 1959). For measurements of [^{14}C]POPC hydrolysis by PLA_2, aliquots of POPC–DOG dispersions were incubated with 54.1 units of PLA_2. The final volume was 190 μL, and the final concentration of POPC was 1.3 mM. The reaction was terminated after 10 min by the addition of EDTA to a final concentration of 0.1 M.

Products of the reactions were separated by thin-layer chromatography. The solvent system was chloroform/methanol/ammonium hydroxide/water (65:25:4:1 v/v) to separate [^{14}C]POPC from its hydrolysis products and chloroform/methanol/ammonium hydroxide (85:15:1 v/v) to separate [^{14}C]DOG from its hydrolysis products. In control experiments, incubations carried out in the absence of the enzymes did not show any lipid hydrolysis nor did those carried out with the enzyme added after the addition of EDTA or chloroform/methanol. The extent of hydrolysis of the radiolabeled substrate was determined as described above, and areas under the peaks were used to calculate the percent hydrolysis for each reaction.

Hydrolysis of Lipid Monolayers. The multiprocessor, interfacial monitor/controller, and monolayer collection techniques used to study the enzymatic hydrolysis of lipid monolayers have been described previously (Tsujita & Brockman, 1987). The present experiments were performed at 15 °C on a subphase of 5 mM PIPES (pH 6.6), 0.1 M sodium chloride, and 0.04% sodium azide. When PLA_2 was used, the subphase also included 2.5 mM $CaCl_2$. The appropriate amount of lipid was spread at low pressure over both compartments of the trough and solvent allowed to evaporate for 3 min. The pressure–area feedback control processor was utilized to compress the monolayer until the final area was 26–27 cm^2, the area was changing less than 1%/min, and the surface pressure was 1–4 mN/m below the collapse pressure for the mixture. After film stabilization, the stirring speed was ramped linearly to 100 rpm over 10 s. For hydrolysis of POPC, 3.3 units of PLA_2 were injected 1 min after stirring was started, and the film was collected on hydrophobic paper (Bhat & Brockman, 1981) 8 min later. For the hydrolysis of DOG, 1834 units of colipase were added at 1 min and 80.9 units of lipase at 11 min, and the film was collected as above after an additional 10 min. The adsorbed lipids were eluted by washing the paper with 11 mL (5.5 + 2.75 + 2.75 mL) of chloroform/methanol (2:1) containing unlabeled substrates and products each at 25 μM. Following solvent evaporation with N_2, the sample was redissolved in a small volume of solvent, unreacted substrates and products were chromatographed, and

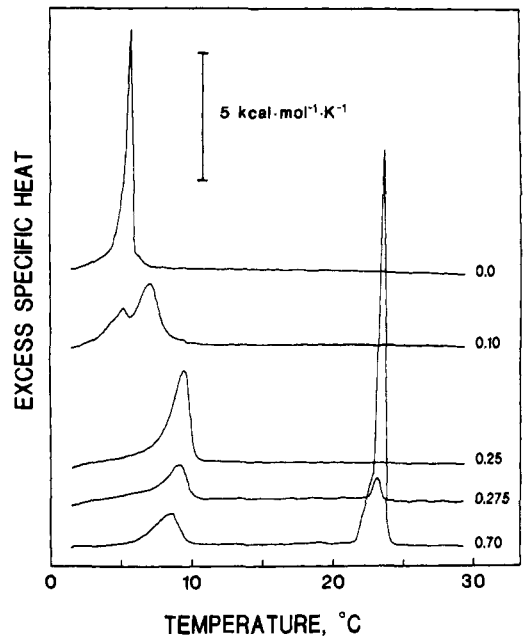

FIGURE 1: Differential scanning colorimetric thermograms for dispersions of SOPC–DOG in excess buffer in the equilibrium state. The mole fraction of DOG is indicated beside each thermogram.

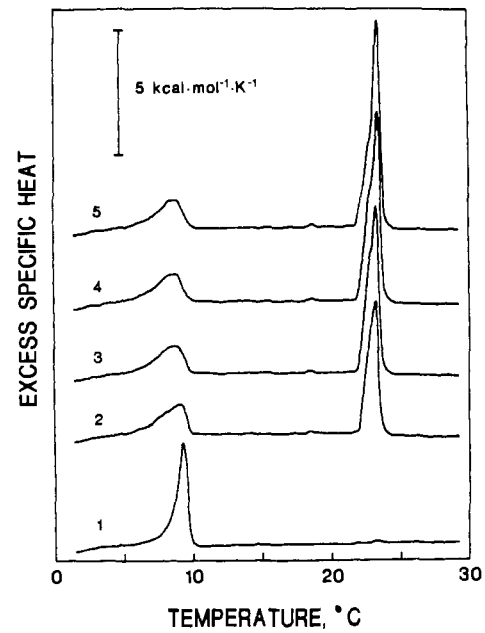

FIGURE 2: Successive differential scanning calorimetric thermograms for a freshly prepared SOPC–DOG dispersion at a DOG mole fraction of 0.5. The scan number is indicated beside each thermogram.

radioactivity was analyzed as described above. Under the conditions which give more than 40% hydrolysis of DOG by lipase, oleic acid is partially soluble and, therefore, is not completely recovered with the monolayer. The substrate/product analysis was not corrected for this small loss. Thus, the results reported reflect a minimum value for the extent of hydrolysis.

RESULTS

To determine the miscibility of DOG and the PC's, the thermotropic phase behavior of DOG–SOPC dispersions was studied. Freshly prepared dispersions were placed in the calorimeter and cooled and heated several times as described under Materials and Methods. SOPC exhibits an acyl chain order–disorder transition at 5.3 °C, and, below 0.25 mole fraction of DOG, all mixtures exhibit two overlapping peaks (Figure 1). These do not change significantly with repeated heating and cooling. The transition temperature for pure SOPC is approximately equal to that previously reported (Davis et al., 1980). The second peak in mixtures shifts to higher temperatures with increasing mole fraction of DOG up to 0.25 and grows at the expense of the SOPC transition peak. At 0.25 mole fraction of DOG, only a single transition at 9.4 °C is observed. Above 0.25 mole fraction of DOG, metastability is observed. As exemplified in Figure 2, the first scan (metastable state) exhibits a single peak at 9.4 °C. The second and consecutive scans (equilibrium state) exhibit two or three peaks: a lower temperature peak at 9.4 °C, a second sharp peak at 23.4 °C, and, in some cases, a very small peak at 18.5 °C. The acyl chain order–disorder phase transition of the β form of DOG is 25 °C (Baily, 1950); therefore, the higher temperature transition is presumed to be the melting of the β form of diolein. This higher temperature peak increases in area with increasing mole fraction of DOG (Figure 1), whereas the area of the 9.4 °C peak remains nearly constant. Even when the temperature was increased to near 100 °C during the first scan, a distinct melting transition for DOG was not observed. The very small peak at 18.5 °C presumably indicates the presence of a small amount of the α form of DOG (Bailey, 1950).

The effect of DOG on the phase transitions of POPC was also investigated (data not shown). In general, observations made for the POPC–DOG system were the same as with the SOPC–DOG system. It has been recently reported that ethylene glycol, widely employed as an antifreeze in calorimetric studies, influences the thermal properties (van Etchteld et al., 1980) and causes acyl chain disordering (Nicolay et al., 1986) in unsaturated phospholipids. Therefore, it was not used, and observations of phase transitions below 0 °C were avoided because of instrument limitations. A single peak beginning below 1 °C and ending by 4 °C was observed for all mole fractions on the first scan. The second and consecutive scans exhibited two or three phase transitions for mole fractions of DOG greater than 0.25: the peak below 4 °C, a very small endotherm at 18.5 °C, and a major endotherm at 23.4 °C.

In order to construct a phase diagram for the system, we first considered the dramatic changes in the transition properties of SOPC–DOG mixtures in the equilibrium state which occur between 0.2 and 0.3 mole fraction of DOG, as shown in Figure 1. By analogy with lipid film behavior (Smaby & Brockman, 1985), we assume that these dramatic changes reflect the formation of a complex or preferred packing array which behaves as a third component in the binary mixture. To calculate the complex composition, X_c, the area under the 23.4 °C peak was compared to the area under the peak at 9.4 °C. This ratio yields a straight line ($r = 0.997$) and when extrapolated to zero gives a complex stoichiometry value of 0.25 mole fraction of DOG (Figure 3). The method of Mabrey and Sturtevant (1976), which includes corrections for transition widths, and X_c calculated above were used to construct the phase diagram for SOPC–DOG dispersions. As shown in Figure 4, it consists of two separate regions. Below X_c, an isomorphous system exists (Cevc & Marsh, 1987). The two lipid components, SOPC and complex, are completely miscible in both the liquid-crystal and gel phases. Above X_c, the complex and DOG are immiscible in both the gel and the liquid-crystal phases since two invariant transitions exist, one at 9.4 °C (the phase transition of the complex) and one at 23.4 °C (the phase transition of DOG). Mixtures at mole fractions of DOG greater than 0.8 were not studied due to difficulties in uniformly dispersing the lipids in buffer.

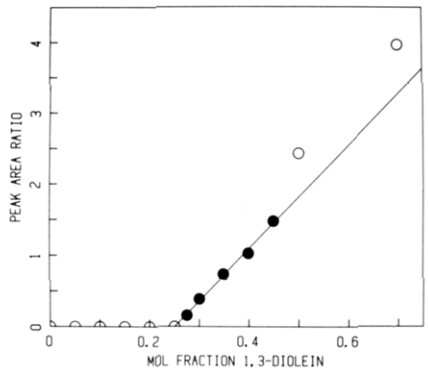

FIGURE 3: Ratio of the area of the melting endotherm for DOG to that of the complex (peak area ratio) as a function of composition for mixtures of DOG and SOPC. The straight line was fitted to the points represented by the closed circles by using a least-squares method.

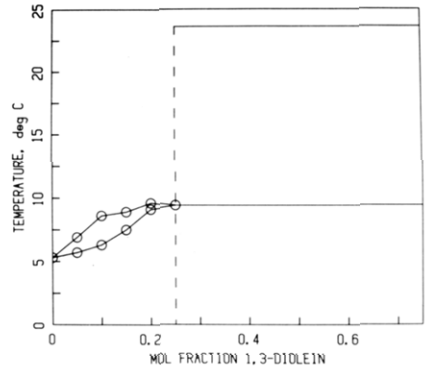

FIGURE 4: Temperature–composition phase diagram for SOPC–DOG dispersions constructed from differential scanning calorimetry data, as in Figure 1, and using X_c determined as outlined under Results.

Freeze–fracture electron microscopy was used to determine the general phase and fracture-face morphologies of SOPC–DOG dispersions. The general phase of the dispersions through 0.65 mole fraction of DOG is multilamellar (Figure 5a–e). A dramatic change in the general morphology of the dispersions occurs at 0.8 mole fraction of DOG (Figure 5f). "Soccer ball"-like particles which appear to be nonlamellar are present with few multilamellar vesicles, and the particle surface is that of an irregular, nonplanar hexagonal array. These particles appear to be aggregates of numerous small particles ranging from 270 to 1200 Å in diameter with the majority being 360 Å. The equilibrium state was not characterized by freeze–fracture electron microscopy because of phase separation of samples containing high mole fractions of DOG. Similar changes in the fracture-face morphology are observed for POPC–DOG dispersions although the "soccer ball"-like particles appear at 0.65 mole fraction of DOG.

DPH fluorescence was used to measure changes in the order of the acyl chains with increasing concentrations of DOG. The fluorescence probe depolarization technique as applied to membrane structure has been previously described (Shinitzky et al., 1971), and the use of DPH as a probe of the hydrocarbon region of lipid bilayers has been described by Shinitzky and Barenholz (1974). DPH fluorescence polarization, at 15 °C, of freshly prepared dispersions was plotted as a function of DOG content as shown in Figure 6. The fluorescence polarization remains constant or increases slightly up to 0.25 mole fraction of DOG. It then decreases continuously with increasing mole fraction of DOG. Freshly prepared POPC–DOG dispersions exhibited a behavior similar to SOPC–DOG dispersions with the exception that the curve was shifted down by approximately 10% (Figure 6).

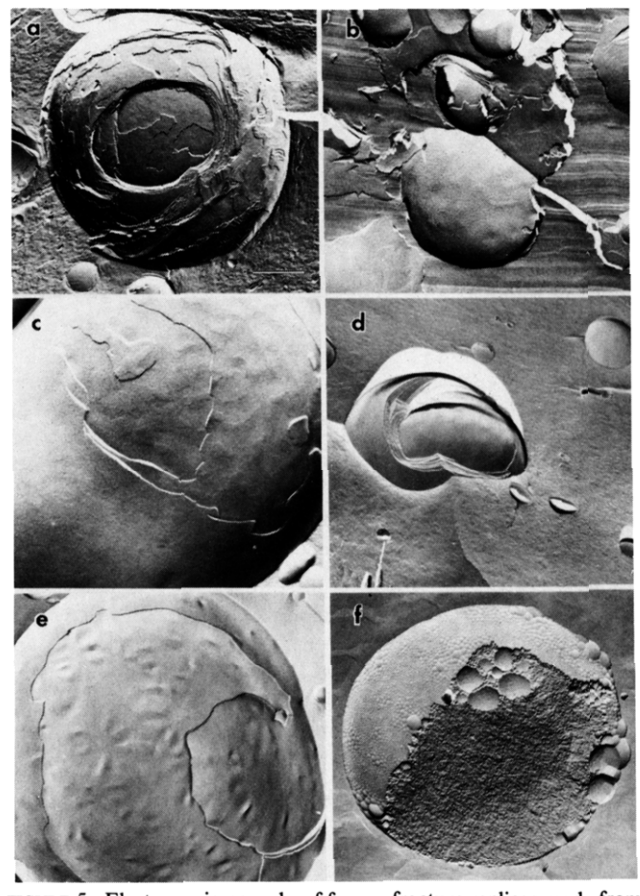

FIGURE 5: Electron micrographs of freeze–fracture replicas made from freshly prepared SOPC–DOG dispersions quenched from 15 °C. The mole fractions of DOG are as follows: (a) 0.0, (b) 0.15, (c) 0.25, (d) 0.4, (e) 0.65, and (f) 0.8. The bar equals 500 nm for all panels.

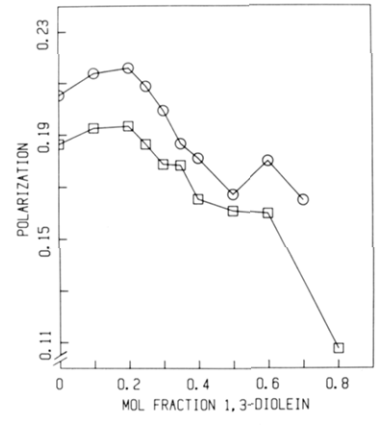

FIGURE 6: Dependence of DPH polarization at 15 °C on DOG content in freshly prepared SOPC–DOG (○) and POPC–DOG (□) dispersions.

In order to study the effect of POPC–DOG interactions on substrate availability, freshly prepared dispersions were subjected to the action of lypolytic enzymes, namely, PLA_2 and pancreatic lipase plus excess colipase. The results are shown in Figure 7. Below 0.25 mole fraction of DOG with freshly prepared bilayers, hydrolysis of the dispersions by PLA_2 remains nearly constant at a value of 5% (Figure 7a). Above 0.25 mole fraction of DOG, there is a dramatic increase in the hydrolysis to approximately 70% with a slight increase at 0.8 mole fraction of DOG. A similar response was observed with lipase (Figure 7b) and with higher concentrations of both enzymes (not shown). At lower concentrations of PLA_2 or lipase, a more gradual increase in hydrolysis occurs above 0.25 mole fraction of DOG. Lipid dispersions subjected to one

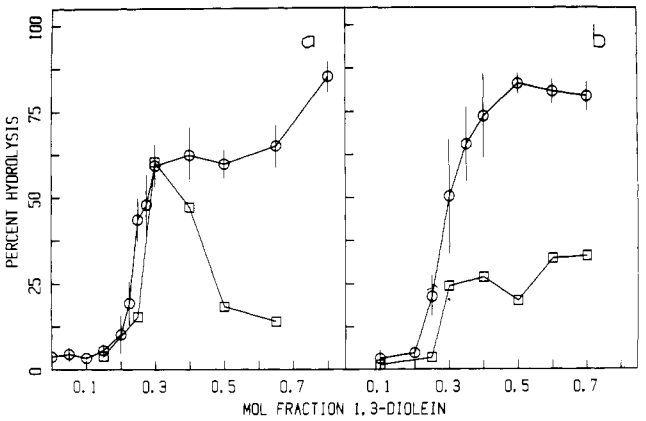

FIGURE 7: Percent substrate hydrolysis at 15 °C for DOG–POPC dispersions. Hydrolysis of (a) POPC by PLA_2 in the equilibrium state (□) and in the metastable state (○) and of (b) DOG by lipase + colipase in the equilibrium state (□) and in the metastable state (○). Vertical lines through data represent ±1 SD for data were obtained at least in triplicate.

heating and cooling cycle, which mimicked the scanning and cooling cycle of the calorimeter, were also exposed to PLA_2 and lipase. The hydrolysis of these lipid dispersions by PLA_2 exhibits an increase between 0.25 and 0.3 mole fraction DOG and then a gradual decrease (Figure 7a). The hydrolysis of heated and cooled POPC–DOG dispersions by lipase below 0.25 mole fraction of DOG is similar to that of the freshly prepared dispersions (Figure 7b). Above 0.25, however, maximal substrate hydrolysis increased to only 25% compared to greater than 75% with freshly prepared dispersions. Lipid dispersions subjected to multiple heating and cooling cycles exhibited the same hydrolysis pattern as those heated and cooled only once.

To determine the miscibility and packing of DOG and SOPC or POPC in surface phases, mixtures of these lipids were characterized in films at the argon/buffer interface. These mixtures were studied at 15 °C, between the acyl chain order–disorder phase transition of the complex and DOG, and at 24 °C, around the DOG chain melting transition. In spite of the proximity of 24 °C to the phase transition temperature of bulk DOG, pure DOG exhibits a continuous surface pressure–area isotherm (Smaby & Brockman, 1985). The phase behavior of these mixtures at interfaces is similar to that which we have previously described (Smaby & Brockman, 1985). For DOG–SOPC mixtures at 24 °C, the phase diagram (Figure 8a) shows a region of monolayer phase (region I) and a region of monolayer coexistence with bulk DOG (region II). For DOG–POPC at 15 and 24 °C, similar phase diagrams were obtained (data not shown). The phase diagram for DOG–SOPC mixtures at 15 °C is slightly more complicated (Figure 8b) although it exhibits a region of monolayer phase (region I) and a region of monolayer–bulk phase coexistence (region II). Phase transitions above 47 mN/m are not well-defined and are presumably the result of acyl chain ordering transitions (Albrecht et al., 1978). Additionally, limited data show that at 18 °C the phase diagram is of the simpler type shown in Figure 8a. These phase diagrams indicate that the formation of preferred packing arrays or complexes is a common property of these DOG–PC mixtures. The point of intersection of the curves in each phase diagram is the mole fraction of DOG at which only complex is present, X_c. The complex stoichiometries were determined as described previously (Smaby & Brockman, 1985) and are 0.24 for POPC at 15 and 24 °C, 0.24 for SOPC at 24 °C, and 0.27 for SOPC at 15 °C (lower transition from Figure 8b).

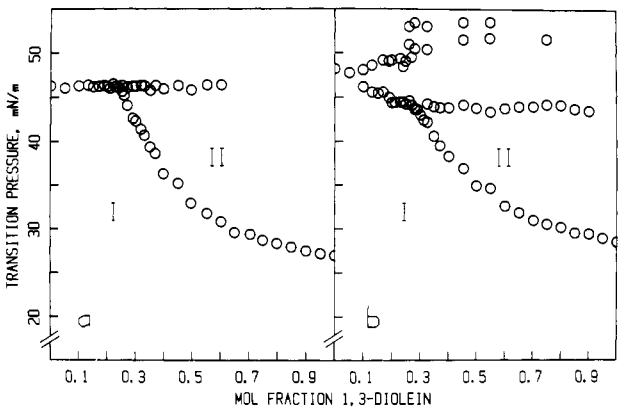

FIGURE 8: Isothermal transition pressure–composition phase diagrams for DOG–SOPC mixed films at (a) 24 °C and (b) 15 °C. Phase transitions were identified as described in the text.

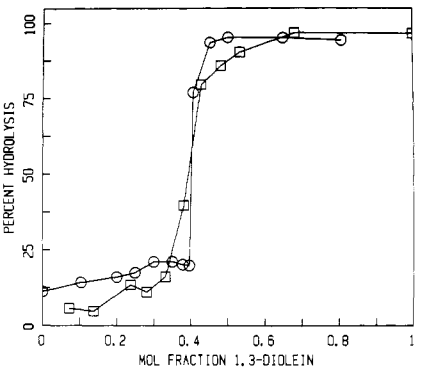

FIGURE 9: Percent substrate hydrolysis at 15 °C as a function of composition for mixtures of DOG and POPC near film collapse. Hydrolysis of POPC by PLA_2 (○) and DOG by lipase plus colipase (□).

The effect of diacylglycerols on the action of lipolytic enzymes was further examined by incorporating DOG into POPC monolayers. The dependence of PLA_2 stimulation on the amount of DOG present in the POPC monolayer is shown in Figure 9. The PLA_2 showed minimal activity toward pure POPC monolayers and monolayers containing up to 0.4 mole fraction of DOG. At 0.4 mole fraction of DOG and higher concentrations, there was a dramatic increase in activity, and most of the substrate was hydrolyzed. A similar pattern of response was observed with lipase. Below 0.4 mole fraction of DOG, lipase showed little activity toward the substrate, but above this concentration of DOG, almost all the substrate was hydrolyzed. At approximately 0.25 mole fraction of DOG, only a small amount of hydrolysis occurs with both enzymes when the pressure is lowered to around 30 mN/m. This is the value where hydrolysis of either substrate is complete for films with 0.8 mole fraction of DOG. This shows that the increase in activity is not due simply to the surface pressure of the films which decreases above 0.25 mole fraction of DOG.

Discussion

To help understand the relation between monolayers and bilayers, the miscibility of DOG and PC in aqueous dispersions and lipid films was examined. The data obtained from differential scanning calorimetry of dispersions suggest that the addition of DOG results in the formation of specific complexes or preferred packing arrays at 0.25 mole fraction of DOG. Earlier studies of similar systems employing NMR and X-ray diffraction failed to detect this complex formation (Das & Rand, 1984, 1986; Dawson et al., 1984). The miscibility behavior of DOG with SOPC or POPC in lipid films at 15

and 24 °C also shows complex formation at mole fractions of DOG ranging from 0.24 to 0.27. In a previous study (Smaby & Brockman, 1985), complex formation was observed for POPC with 1,2- and 1,3-diolein in films at 24 °C and was 0.25 mole fraction of diolein in each case. The similarity of the complex stoichiometries in both monolayers and bilayers suggests that the complex or "pseudo compound" is structurally similar in both systems. As noted previously, this is most likely a two-dimensional array and not a stoichiometric complex in the chemical sense. However, the temperature and phase independence of the complex composition in both systems indicates that the array has a defined composition, i.e., that the free energy of interactions between the lipids is strong relative to that for the thermotropic transitions of the acyl chains. This invariance of composition over a range of temperatures is also shown semiqualitatively by the temperature–composition phase diagrams determined for diacylglycerol–PC mixtures using X-ray diffraction (Das & Rand, 1986). Previously, Smaby and Brockman (1985) have suggested that the composition of such preferred packing arrays is determined by interactions involving the more polar moieites of DOG and PC. This is also supported by a recent monolayer study determining the miscibility of DOG with a series of PC's and other phospholipids (B. A. Cunningham, J. Smaby, and H. L. Brockman, unpublished results).

Freeze–fracture electron microscopy indicates that the complex is lamellar (Figure 5c). This confirms earlier results obtained with less well-characterized PC–diacylglycerol dispersions. In this composition and temperature range, only lamellar structures were observed using NMR, X-ray diffraction, and freeze-etching techniques (Das & Rand, 1984, 1986; Dawson et al., 1984). Several observations suggest that complex formation may have a stabilizing effect on the structure of PC–DOG bilayers and monolayers. One indication is the transition temperature of the bilayer complex which is higher than for SOPC or POPC alone. For the monolayer systems at 24 °C and for POPC–DOG at 15 °C, the collapse surface pressure of the complex is the same as for the pure PC instead of being intermediate between the collapse pressure of the PC and the lower collapse pressure of DOG. This represents a stabilization of the system at the complex composition relative to ideal mixing of the components and indicates a surface free energy per centimeter squared at least as low as that of the PC alone. The fluorescence polarization of DPH (Figure 6) appears to increase slightly with complex formation. Kawato et al. (1977) have proposed that DPH fluorescence polarization should be a direct function of an acyl chain order parameter, consistent with the calorimetry data. At the complex composition, lipolytic activity is not enhanced, suggesting the absence of the type of destabilizing structures known to promote lipolysis [e.g., see Dawson (1982) and references cited therein]. While no one of these experiments is definitive, together they do suggest an ordering and possible thermodynamic stabilization of the system at the complex composition relative to SOPC or POPC alone.

In the region of DOG mole fractions between 0.0 and X_c, phospholipid and complex coexist. Bulk DOG does not phase-separate upon repeated heating and cooling, and the endotherms are reproducible. Neither is there any evidence at the collapse of the mixed monomolecular films for formation of a bulk DOG phase (Smaby & Brockman, 1985). Similar monolayer data for this region have been analyzed by using the two-dimensional phase rule (Smaby & Brockman, 1988). This indicates that in either the monolayer phase or the presumed bilayer phase formed upon monolayer collapse, complex and PC must be immiscible. In which phase the required immiscibility occurs could not be directly determined. Examination of the calorimetric scans at compositions intermediate between 0.0 and X_c (Figure 1) shows what appear to be two overlapping peaks. This suggests the immiscibility of complex and PC, i.e., each peak represents the melting of one of the species. Immiscibility of the components, however, violates the three-dimensional phase rule (Mabrey & Sturtevant, 1976). Moreover, the continuous change with DOG composition of the onset and completion temperatures shown in the phase diagram (Figure 4) and the peak broadening at intermediate compositions (Figure 1) suggest miscibility. A similar system has been described by Mabrey and Sturtevant (1976). Such behavior is likely due to the formation of relatively stable domains of complex and PC in a single phase. Such domains may contain up to several hundred molecules of lipid (Mabrey & Sturtevant, 1977). Thus, complex and PC may coexist as stable domains in both the gel and liquid-crystalline phases, making the system intermediate in miscibility behavior. This type of macroscopic miscibility–microscopic immiscibility can explain why the analysis of monolayer data noted above requires immiscibility. At a temperature of 24 °C, SOPC, POPC, and their complexes with DOG are clearly in the liquid-crystalline state. The onset of monolayer collapse detected experimentally could be from a mixture of monolayer domains or due to a mixture of bilayer domains.

At DOG mole fractions greater than X_c, dispersions with either SOPC or POPC exhibit metastability; a single phase transition is detected by differential scanning calorimetry on the first scan, and multiple transitions are observed thereafter. Freeze–fracture electron microscopy of SOPC–DOG dispersions indicates that the metastable state is lamellar up to about 0.6–0.8 mole fraction of DOG (Figure 5c–e). Upon heating and cooling, phase separation occurs to give a diolein bulk phase, or emulsion, and complex (Figure 1), which also appears lamellar. Thus, a lamellar phase is present in both states. This is generally consistent with earlier X-ray diffraction results obtained at 15 °C for a similar system, although the phase diagram is void of data in part of this region (Das & Rand, 1986). Using NMR and freeze-etching, a pure hexagonal phase has been observed at 50 mol % mixed diacylglycerols in yeast PC. However, these studies were performed at 37 °C (Dawson et al., 1986) where X-ray also shows the hexagonal phase at this composition.

The formation of the metastable state can be related to the phase diagrams obtained for PC–DOG films (Figure 8). Consider a monolayer with a DOG composition greater than X_c, e.g., 0.6, and an initial surface pressure in region I (Figure 8a). Compression of the film will increase the surface pressure without any phase change until the surface pressure corresponding to the region I–region II boundary is encountered. Continued compression causes formation of a bulk diolein phase (region II of Figure 8a), and, hence, the DOG composition of the monolayer phase in region II must decrease. At any surface pressure in region II, the composition of the monolayer phase is the value of the abscissa corresponding to the same pressure on the region I–region II boundary. Continued compression of the film ultimately yields a surface phase composition and pressure equal to those of the complex, and no more DOG can be expelled. This point is on the line which defines the upper limit of region II at the initial system composition, e.g., 0.6. Additional compression of the film does not change the surface pressure and forms a nonmonolayer, presumably bilayer, phase which has the composition of the

complex. Because the surface pressure is the decrease in surface free energy per centimeter squared due to lipid, the surface free energy at the point of crossing the region I–region II boundary will be greater than that at the upper boundary of region II (Figure 8a). Comparison of the phase behavior of monolayers and dispersions suggests that the point at which the region I–region II boundary is encountered, i.e., the monolayer collapse pressure, is analogous to the metastable, higher energy bilayer state which exists between X_c and DOG compositions of 0.6–0.8 for SOPC (Figure 5d) and 0.65 for POPC. Heating and cooling cause a relaxation to two phases; a bulk diolein phase, or emulsion, and a bilayer phase of complex (Figure 1).

Support for this hypothesis comes from comparison of the enzymatic studies. Hydrolysis of mixed monomolecular films at pressures near the upper limit of region I (Figure 9) showed a pronounced increase at about 0.4 mole fraction of DOG. An earlier study of PC hydrolysis by PLA_2 using medium-chain triglyceride–PC mixed films at lower surface pressures showed qualitatively similar composition-dependent activity changes (Pieroni & Verger, 1983). Hydrolysis of metastable, PC–DOG bilayers showed the same type of composition dependence (Figure 7) as did monolayer hydrolysis (Figure 9), although it was less abrupt and began at 0.25–0.3 mole fraction of DOG. Such quantitative differences point out that the monolayer and dispersion systems may be similar or related but not necessarily identical. Additionally, the bilayers show size heterogeneity, and, hence, there are different radii of particle curvature. Heating and cooling of the metastable phase at DOG mole fractions above X_c produce a bilayer phase of complex. Because complex is not readily hydrolyzed in monolayers, the heated and cooled bilayers should become refractory to hydrolysis. Figure 7 shows that this is the case although loss of activity is not complete. Considering the particular nature of the dispersion system and the size heterogeneity of the particles, a lack of complete and ideal phase redistribution is reasonable. Unilamellar bilayers of uniform size would provide a better model, but we were unable to make them with compositions above X_c because of macroscopic phase separation. Earlier reports of the activity of other phospholipases toward PC–DOG dispersions (Dawson et al., 1983, 1984; Buckley, 1985) showed results nearly identical with those we obtained using PLA_2 with heated and cooled dispersions. This suggests that the preparations used in those studies were not in the metastable state but had phase-separated. The fluorescence polarization measurements also support the phase analogy. Along the region I–region II phase boundary at mole fractions of DOG above X_c, the average area per fatty acyl chain increases with increasing DOG at 15 °C (data not shown), as well as at 24 °C (Smaby & Brockman, 1985). This correlates well with the observed DOG-dependent decrease in polarization above X_c (Figure 6).

Above 0.6–0.8 mole fraction of DOG, novel metastable structures are observed by electron microscopy. They appear to be clusters of droplets or dodecahedra, although some, e.g., Figure 5f, fracture through the particle, as do emulsions (Wong et al., 1987) to reveal a granular interior. Studies of PC–diacylglycerol dispersions using X-ray diffraction indicate the formation of a cubic phase in this region (Das & Rand, 1986) which could be the precursor or product of these structures.

In spite of the fact that lipid monolayers are constrained to a macroscopically planar state, we observe a high degree of internal consistency and similarity in the behavior of DOG–PC mixtures in model monolayers and aqueous lipid dispersions. Thus, the composition phenomena, such as complex formation, are presumed to occur also in native membranes. With respect to the enzymatic studies, the ability to turn on or off hydrolysis, i.e., an amplification of response in which a small increment in stimulus leads to a large change in output, is an essential feature of many biochemical processes. Koshland (1987) has termed such phenomena ultrasensitive, that is, generating a steep sigmoid curve rather than a discontinuity; a zero-order ultrasensitive system may require only a small change in substrate to go from 10 to 90% activity, which is observed in our systems. These changes demonstrate, in principle, how the generation of diacylglycerols in membranes can trigger subsequent hydrolysis of phospholipid by an intracellular PLA_2 and how a diacylglycerol lipase could be triggered to turn off a diacylglycerol signal. Because this form of regulation occurs as a consequence of lipid–lipid interactions, it is also expected that complex formation and its influence on lipid packing will play a role in other processes occurring at membrane–water interfaces.

ACKNOWLEDGMENTS

We thank N. K. Mizuno, W. E. Momsen, and J. M. Smaby for their technical assistance. Freeze–fracture was provided by the Electron Microscopy Core and fluorescence spectroscopy equipment by the Spectroscopy Core of Program Project Grant HL08214.

REFERENCES

Albrecht, O., Gruler, H., & Sackman, E. (1978) *J. Physiol. (Paris) 39*, 301–313.

Bailey, A. E. (1950) in *Melting and Solidification of Fats*, pp 117–180, Wiley-Interscience, New York.

Bartlett, G. R. (1959) *J. Biol. Chem. 234*, 466–468.

Berridge, M. J., & Irvine, R. F. (1984) *Nature (London) 312*, 315–321.

Bhat, S. G., & Brockman, H. L. (1981) *J. Biol. Chem. 256*, 3017–3023.

Bligh, E. G., & Dyer, W. J. (1959) *Can. J. Biochem. Physiol. 37*, 911–917.

Brockman, H. L., Jones, C. J., Schwebke, C. J., Smaby, J. M., & Jarvis, D. E. (1980) *J. Colloid Interface Sci. 78*, 502–512.

Brockman, H. L., Smaby, J. M., & Jarvis, D. E. (1984) *J. Phys. E. 17*, 351–353.

Buckley, J. T. (1985) *Can. J. Biochem. Cell Biol. 63*, 263–267.

Burch, R. M. (1988) *FEBS Lett. 234*, 283–286.

Cabot, C. M., Welsh, C. J., Cao, H. T., Zhang, Z. C., & Chabbott, H. (1988) *FASEB J. 2*, A1364.

Canioni, P., Julein, R., Rathelot, J., Rochat, H., & Sarda, L. (1977) *Biochimie 59*, 919–925.

Cevc, G., & Marsh, D. (1987) in *Phospholipid Bilayers: Physical Principles and Models*, pp 369–406, Wiley-Interscience, New York.

Chapus, C., Desnuelle, P., & Foglizzo, E. (1981) *Eur. J. Biochem. 115*, 99–105.

Das, S., & Rand, R. P. (1984) *Biochem. Biophys. Res. Commun. 124*, 491–496.

Das, S., & Rand, R. P. (1986) *Biochemistry 25*, 2882–2889.

Davis, P. J., Coolbear, K. P., & Keough, K. M. (1980) *Can. J. Biochem. 58*, 851–858.

Dawson, R. M. C. (1982) *J. Am. Oil Chem. Soc. 59*, 401–406.

Dawson, R. M. C., Hemington, N. L., & Irvine, R. F. (1983) *Biochem. Biophys. Res. Commun. 117*, 196–201.

Dawson, R. M. C., Irvine, R. F., Bray, J., & Quinn, P. J. (1984) *Biochem. Biophys. Res. Commun. 125*, 836–842.

de Haas, G. H., Posterna, N. M., Nieuwenhuizen, W., & van Deenen, L. L. M. (1968) *Biochim. Biophys. Acta 159*, 103–117.

Erlanson, C., & Borgström, B. (1972) *Biochim. Biophys. Acta 271*, 400-412.
Kawato, S., Kinosita, K., & Ikegami, A. (1977) *Biochemistry 16*, 2319-2324.
Kolesnick, R. N. (1987) *J. Biol. Chem. 262*, 16759-16762.
Kolesnick, R. N., & Paley, A. E. (1987) *J. Biol. Chem. 262*, 9204-9210.
Kolesnick, R. N., & Clegg, S. (1988) *J. Biol. Chem. 263*, 6534-6537.
Koshland, D. E. (1987) *Trends Biochem. Sci. (Pers. Ed.) 12*, 225-229.
Mabrey, S., & Sturtevant, J. M. (1976) *Proc. Natl. Acad. Sci. U.S.A. 73*, 3862-3866.
Mabrey, S., & Sturtevant, J. M. (1977) *Biochim. Biophys. Acta 486*, 444-450.
Majerus, P. W., Neufeld, E. J., & Wilson, D. B. (1984) *Cell (Cambridge, Mass.) 37*, 701-703.
Momsen, W. E., & Brockman, H. L. (1978) *J. Lipid Res. 19*, 1032-1037.
Morrissey, J. H. (1981) *Anal. Biochem. 117*, 307-310.
Nicolay, K., Smaal, E. B., & de Kruijff, B. (1986) *FEBS Lett. 209*, 33-36.
Nieuwenhuizen, W., Kunze, H., & de Haas, G. H. (1974) *Methods Enzymol. 32*, 147-154.
Nishizuka, Y. (1986) *Science (Washington, D.C.) 233*, 305-312.
Perrin, D. D., Armarego, W. L. F., & Perrin, D. R. (1966) in *Purification of Laboratory Chemicals*, pp 156-158, Pergamon, New York.
Pieroni, G., & Verger, R. (1983) *Eur. J. Biochem. 132*, 639-644.
Rudd, E. A., Mizuno, N. K., & Brockman, H. L. (1987) *Biochim. Biophys. Acta 918*, 106-114.
Shinitzky, M., & Barenholz, Y. (1974) *J. Biol. Chem. 249*, 2652-2657.
Shinitzky, M., Dianoux, A. C., Gitler, C., & Weber, G. (1971) *Biochemistry 10*, 2106-2113.
Smaby, J. M., & Brockman, H. L. (1985) *Biophys. J. 48*, 701-708.
Smaby, J. M., & Brockman, H. L. (1988) *J. Lipid Res. 28*, 1078-1087.
Smaby, J. M., Hermetter, A., Schmid, P. C., Paltauf, F., & Brockman, H. L. (1983) *Biochemistry 22*, 5808-5813.
Tsujita, T., & Brockman, H. L. (1987) *Biochemistry 26*, 8423-8429.
Van Etchteld, C. J. A., de Kruijff, B., & de Gier, J. (1980) *Biochim. Biophys. Acta 595*, 71-81.
Verger, R., Sarda, L., & Desnuelle, P. (1971) *Biochim. Biophys. Acta 242*, 580-591.
Wolfe, D. H., & Brockman, H. L. (1988) *Proc. Natl. Acad. Sci. U.S.A. 85*, 4285-4289.
Wong, K. F., Parmar, Y. I., Mayer, L. D., Pritchard, P. H., & Cullis, P. R. (1987) *Biochim. Biophys. Acta 921*, 411-414.

Conformational States of the Nicotinic Acetylcholine Receptor from *Torpedo californica* Induced by the Binding of Agonists, Antagonists, and Local Anesthetics. Equilibrium Measurements Using Tritium–Hydrogen Exchange†

Michael P. McCarthy and Robert M. Stroud*
Department of Biochemistry and Biophysics, University of California, San Francisco, California 94143-0448
Received May 23, 1988; Revised Manuscript Received August 12, 1988

ABSTRACT: The tritium–hydrogen exchange kinetics of *Torpedo californica* AChR, in native membrane vesicles at pH 7.4 and 0 °C, have been analyzed in the presence of agonists, partial agonists, local anesthetics, and competitive antagonists. The agonists carbamylcholine (10 μM–1 mM) and suberyldicholine (10 μM) and the partial agonists decamethonium (25 μM and 1 mM) and hexamethonium (1 mM) have no effect on the exchange kinetics, although at lower concentration carbamylcholine may slightly accelerate exchange. Nondesensitizing local anesthetics do affect the exchange behavior, dependent on concentration. Procaine at 500 μM moderately retards exchange while procaine at 10 mM and tetracaine at 5 mM slightly accelerate exchange. The competitive antagonist α-bungarotoxin retards exchange significantly, as does *d*-tubocurarine although to a lesser extent. These results suggest that the resting and desensitized conformations of the AChR are very similar in overall solvent accessibility and that at lower concentrations noncompetitive blockers such as procaine may stabilize a less solvent-accessible state of the AChR. The competitive antagonists α-bungarotoxin and *d*-tubocurare also stabilize a dynamically restricted, less solvent-accessible conformation of the acetylcholine receptor, demonstrating that a large conformational change accompanies binding of these toxins. Any change in conformation which may accompany desensitization is very different from these effects.

Tritium–hydrogen exchange provides a powerful measure of any change in secondary structure or solvent accessibility that accompanies ligand binding, or other alteration in state of a macromolecule. In principle, the method is of very high resolution, once individual amides which undergo change are assigned. We report here the initial low-resolution use of this global probe applied to structural and functional changes of the acetylcholine receptor (AChR).[1] The nicotinic AChR

† Supported by National Institutes of Health Fellowship GM-09827 to M.P.M. and by National Institutes of Health Grant GM-24485 and National Science Foundation Grant DMB8615712 to R.M.S.

0006-2960/89/0428-0040$01.50/0 © 1989 American Chemical Society